Eur. Phys. J. E (2023)46:79
https://doi.org/10.1140/epje/s10189-023-00335-1

THE EUROPEAN PHYSICAL JOURNAL E

Regular Article - Soft Matter

Fluctuations, structure, and size inside coacervates

Murugappan Muthukumar[a]

Department of Polymer Science and Engineering, University of Massachusetts, Amherst, MA 01003, USA

Received 5 July 2023 / Accepted 18 August 2023

Abstract Aqueous solutions of oppositely charged macromolecules exhibit the ubiquitous phenomenon of coacervation. This subject is of considerable current interest due to numerous biotechnological applications of coacervates and the general premise of biomolecular condensates. Towards a theoretical foundation of structural features of coacervates, we present a field-theoretic treatment of coacervates formed by uniformly charged flexible polycations and polyanions in an electrolyte solution. We delineate different regimes of polymer concentration fluctuations and structural features of coacervates based on the concentrations of polycation and polyanion, salt concentration, and experimentally observable length scales. We present closed-form formulas for correlation length of polymer concentration fluctuations, scattering structure factor, and radius of gyration of a labelled polyelectrolyte chain inside a concentrated coacervate. Using random phase approximation suitable for concentrated polymer systems, we show that the inter-monomer electrostatic interaction is screened by interpenetration of all charged polymer chains and that the screening length depends on the individual concentrations of the polycation and the polyanion, as well as the salt concentration. Our calculations show that the scattering intensity decreases monotonically with scattering wave vector at higher salt concentrations, while it exhibits a peak at intermediate scattering wave vector at lower salt concentrations. Furthermore, we predict that the dependence of the radius of gyration of a labelled chain on its degree of polymerization generally obeys the Gaussian chain statistics. However, the chain is modestly swollen, the extent of which depending on polyelectrolyte composition, salt concentration, and the electrostatic features of the polycation and polyanion such as the degree of ionization.

1 Introduction

Concentration fluctuations in solutions of uniformly charged polyelectrolytes can be very strong resulting in several structural and thermodynamic features that are not observed in uncharged systems, as revealed in the pioneering work of Fyl Pincus and collaborators [1]. The concept of double screening [2–4], that is the confluence of the Edwards screening [5–8] of short-ranged excluded volume interactions and the Debye screening of the long-ranged electrostatic interactions [9], results in the special properties of polyelectrolyte solutions, such as the spontaneous selection of finite-size structures (structure factor exhibiting a peak at non-zero scattering wave vectors) [2,10–14]. In the presence of multivalent counterions, polyelectrolyte solutions undergo phase separation relatively easily compared to the situation with monovalent counterions [15–17]. The extreme example of multivalent counterions is an oppositely charged polyelectrolyte. When two oppositely charged polyelectrolytes are mixed in an aqueous solution, they can spontaneously form inter-molecular complexes and undergo liquid-liquid phase separation, broadly classified as coacervation [18–59]. In this tribute to Fyl Pincus' long-standing contributions to polyelectrolyte physics, we address concentration fluctuations inside coacervate phases and derive closed-form formulas for correlation length of concentration fluctuations, structure factor, and size of labelled chains in terms of relevant experimental variables.

Starting from the initial experimental observation [18] eight decades ago, the phenomenon of coacervate complexation in a mixture of polycations and polyanions has a long history [19–59]. There are several reviews on this subject providing excellent summary of various experimental results, theoretical approaches, and simulation results [11,57–59]. Furthermore, there is a rapidly growing literature on liquid-like droplets of biocondensates reminiscent of coacervates from synthetic polyelectrolytes [60–69]. The primary theoretical approach to address the coacervate structures and phase diagrams is based on a mean-field argument originally introduced by Voorn and Overbeek [19,20]. As

It is a great pleasure for the author to dedicate this article to Fyl Pincus, whose pioneering research on polymer physics has inspired many polymer scientists, in appreciation of his warm collegiality, inspiration, and friendship.

[a] e-mail: muthu2346@gmail.com (corresponding author)

Published online: 08 September 2023

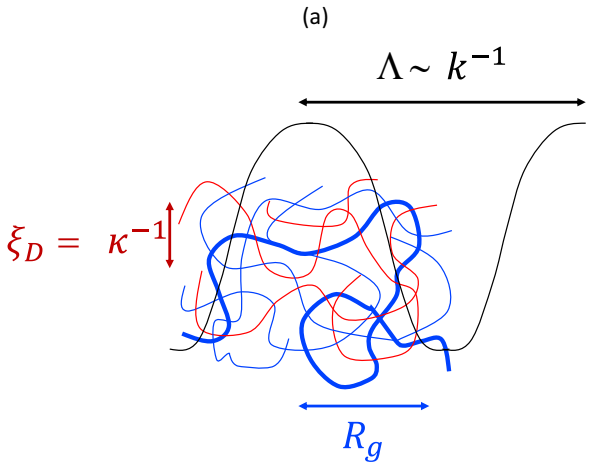

(b)

Case	kR_g	$k\xi_D$
(i)	< 1	< 1
(ii)	< 1	> 1
(iii)	> 1	< 1
(iv)	> 1	> 1

Fig. 1 **a** Sketch of length scales denoting R_g, ξ_D, and the proble length Λ (for $k\xi \ll 1$). A labelled chain is depicted with thick contour. **b** Four experimental conditions to determine structure and size inside coacervates

a deviation from the classical approach towards understanding coacervation phase behavior, only recently, the role of correlations among the inter-chain dipoles (ion-pairs) on coacervation has been addressed [11,53,54].

In parallel, several experimental techniques such as neutron scattering, conductivity measurements, electron microscopy, and thermodynamic analysis, have been used to discern the structure and radius of gyration of a labelled polyelectrolyte chain inside coacervates [29,30,36,37,41,50,52]. The experimental results show that the coacervate is a liquid, rubbery, or glassy, and that a labelled chain adopts either a self-avoiding walk (SAW) or Gaussian statistics, all depending on the system-specific experimental conditions [37,50]. To date, there is no firm theoretical basis to address concentration fluctuations in dense coacervates in terms of strength and range of such correlations and their consequences on the effective inter-segment electrostatic interaction mediated by topologically correlated charged polyelectrolytes, and the size of a labelled chain. A theoretical attempt to address these issues is the primary goal of this paper.

In general, there are four important length scales in the system [2], namely, the Bjerrum length (ℓ_B), correlation length (ξ) for concentration fluctuations, the Debye length ($\xi_D \equiv \kappa^{-1}$), and the radius of gyration (R_g) of a labelled chain, in addition to the monomer length ℓ. The Bjerrum length denotes the strength of the electrostatic interaction in the solution. It is the length at which the electrostatic interaction between two monovalent charges is the thermal energy k_BT (the Boltzmann constant times the absolute temperature). The Debye length denotes the range of electrostatic interaction. ξ, ξ_D, and R_g depend on the composition of the system. Let the total polymer concentration in the coacervate be $c(= c_1 + c_2)$, where c_1 and c_2 are, respectively, the monomer concentrations of the first polyelectrolyte of degree of polymerization N_1, and that of the oppositely charged second polyelectrolyte of degree of polymerization N_2. Let the concentration of the low molar mass monovalent electrolyte in the system be c_s. The correlation length ξ and the radius of gyration R_g depend on c, c_s, N_1, N_2, and ℓ_B, as well as the solvent quality represented by the Flory-Huggins parameter χ. The Debye length ξ_D depends inversely on the square root of the total concentration of fully dissociated small ions. Since a major driving force for complexation between oppositely charged polyelectrolytes is the release of adsorbed counterions from the participating polyelectrolyte chains [28], the total concentration of dissociated small ions participating in the electrostatic screening is roughly $(c_1 + c_2 + c_s)$. Here, the prefactors in front of c_1 and c_2 depend on the degree of counterion adsorption on the parent polyelectrolyte chains, which in turn depends on specific experimental conditions.

In addition to the above mentioned two length scales of ξ and R_g characterizing specific coacervates, the key length scale in scattering experiments that probe coacervates is the probe length $\Lambda \sim k^{-1}$, where k is the scattering wave vector. Experimental determination of ξ and R_g as functions of c, c_s, N_1, N_2, and T depends crucially on the appropriate tuning of the probe length. These three length scales are cartooned in Fig. 1a. Depending on the relation among $\xi_D \equiv \kappa^{-1}, R_g$, and $\Lambda \sim k^{-1}$, four regimes ($kR_g<1, kR_g>1, k\xi_D<1, k\xi_D>1$) arise as shown in Fig. 1b. We present below formulas for ξ and R_g in these four regimes.

Generally speaking, there are three concentration regimes as illustrated in Fig. 2. for consideration of ξ and R_g [2,6,7]. Considering the concentration c_1 of the first polyelectrolyte (either polycation or polyanion), with the corresponding N_1-dependent overlap concentration $c_1^\star$, these regimes are dilute (for $c_1<c_1^\star$), semidilute (for $c_1^\star<c_1<c_1^{\star\star}$), and concentrated (for $c_1>c_1^{\star\star}$). As well known for polyelectrolyte solutions [2,3,11], the concentration fluctuations are strong in the semidilute regime and weak in the concentrated regime, with $c_1^{\star\star}$ being the boundary between the regimes. Analogously, these three regimes exist also for the second polyelectrolyte. For the symmetric case ($N_1 = N_2$), these three regimes are portrayed in Fig. 2, where the polymer concentration c is the total concentration from both polyelectrolytes ($c = c_1 + c_2$).

In dilute solutions containing sufficient added salt or dissociated counterions, the chains are expected to be far from each other and each chain behaving like a self-avoiding walk (SAW) chain. As the polymer concentration increases in the dilute regime, the radius of

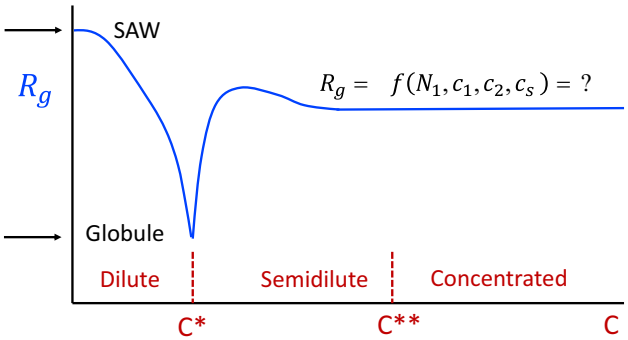

Fig. 2 **a** Sketch of the concentration dependence of the radius of gyration R_g of a labelled chain in a symmetric mixture ($N_1 = N_2$) of polycations and polyanions in the presence of added salt. c is the total polymer concentration. $c^\star$ and $c^{\star\star}$ denote the overlap concentration and the concentration boundary between the regimes of strong fluctuations ($c^\star < c < c^{\star\star}$) and weak fluctuations ($c > c^{\star\star}$). In the dilute regime, chains shrink from self-avoiding walk conformation to globule-like conformation as c increases. The chain re-swells upon an increase in c to reach an asymptotic value for $c > c^{\star\star}$

gyration of a labelled chain is expected to decrease due to formation of branched structures from inter-chain binding among oppositely charged polymers, eventually reaching a globular conformation [11]. Once c is higher than the overlap concentration $c^\star$, the chains would interpenetrate into each other. As a result, we expect the R_g of a labelled chain to be higher than its value at $c \leq c^\star$. Therefore, the chain is expected to re-swell into swollen conformations in the semidilute regime. Upon further increase in c into the concentrated regime, the concentration fluctuations become weak and theoretical methods equivalent to the random phase approximation (RPA) can be implemented for investigating structure and fluctuations in concentrated coacervates. Based on the above expectations, the R_g of a labelled chain is a function of N_1, c, and c_s, as indicated in Fig. 2.

If the temperature is low enough (equivalently ℓ_B is high enough), the ion-pairs formed by oppositely charged monomers are strong so that highly branched structures [11] would form. For such experimental conditions, the coacervates would possess internal microstructures [61,67]. On the other hand, if the temperature is high enough, but below the critical temperature T_c for liquid-liquid phase separation, then the coacervate is expected to be liquid-like without substantial branched architectures. In the present paper, we address only this state of coacervates. Furthermore, we assume that the polymer concentration of the coacervate is high enough to guarantee only weak concentration fluctuations. Using an analytical treatment of a field-theoretic representation of coacervates, we show that the static structure factor exhibits a peak in terms of the scattering wave vector and that the radius of gyration of a labelled chain obeys Gaussian chain statistics with only modest swelling contributed by concentrations of the polyelectrolytes and added salt.

The rest of the paper is organized as follows. The theoretical model is presented in Sect. 2. After introducing theoretical framework in Sect. 3, results based on mean field theory and fluctuations are derived in Sects. 4 and 5, followed by calculations of the structure factor in Sect. 6 for the four cases in Fig. 1b. The effective inter-segment interaction for a labelled chain is derived in Sect. 7, followed by a calculation of the radius of gyration of a labelled chain in Sect. 8. The main results are summarized in the last section.

2 Model

Consider a system of n_1 flexible polycations each containing N_1 segments, n_{1c} counterions of the polycation chains, n_2 flexible polyanions each containing N_2 segments, n_{2c} counterions of the polyanion chains, n_γ ions of species γ from dissolved salt, and n_s solvent molecules in volume V. Let α be the fixed degree of ionization per chain, for both polycations and polyanions, so that each segment of the chains carries a charge of ez_p where e is the electronic charge. The total number of counterions is $n_c = \alpha z_p(n_1 N_1 + n_2 N_2)/z_c$ where z_c is the valency of the both kinds of counterions. Let ez_i be the charge of the i-th charged species. We represent the polycation and polyanion chains as continuous curves of length $L_1 = N_1\ell$ and $L_2 = N_2\ell$, respectivly, where ℓ is the Kuhn step length. The Helmholtz free energy F of the system is given by

$$e^{-\frac{F}{k_B T}} = \frac{1}{n_1! n_2! n_{1c}! n_{2c}! n_s! \prod_\gamma n_\gamma!} \int \prod_{\alpha=1}^{n_1} \mathcal{D}[\mathbf{R}_\alpha] \int \prod_{\beta=1}^{n_2} \mathcal{D}[\mathbf{R}_\beta] \int \prod_i^{n_c+n_s+\sum_\gamma n_\gamma} \mathrm{d}\mathbf{r}_i \times \exp\left[-\mathcal{L}_\alpha - \mathcal{L}_\beta - U - U_b\right], \quad (1)$$

where

$$\mathcal{L}_\alpha = \exp\left[-\frac{3}{2\ell^2}\sum_{\alpha=1}^{n_1}\int_0^{N_1} \mathrm{d}s_\alpha \left(\frac{\partial \mathbf{R}_\alpha(s_\alpha)}{\partial s_\alpha}\right)^2\right], \quad (2)$$

$$\mathcal{L}_\beta = \exp\left[-\frac{3}{2\ell^2}\sum_{\beta=1}^{n_2}\int_0^{N_2} \mathrm{d}s_\beta \left(\frac{\partial \mathbf{R}_\beta(s_\beta)}{\partial s_\beta}\right)^2\right], \quad (3)$$

$$U = \frac{1}{2}\sum_{\alpha=1}^{n_1}\sum_{\alpha'=1}^{n_1}\int_0^{N_1} \mathrm{d}s_\alpha \int_0^{N_1} \mathrm{d}s_{\alpha'} U_{\alpha\alpha'}[\mathbf{R}_\alpha(s_\alpha) - \mathbf{R}_{\alpha'}(s_{\alpha'})] + \frac{1}{2}\sum_{\beta=1}^{n_2}\sum_{\beta'=1}^{n_2}\int_0^{N_2} \mathrm{d}s_\beta \int_0^{N_2} \mathrm{d}s_{\beta'} U_{\beta\beta'}[\mathbf{R}_\beta(s_\beta) - \mathbf{R}_{\beta'}(s_{\beta'})] + \sum_{\alpha=1}^{n_1}\sum_{\beta=1}^{n_2}\int_0^{N_1} \mathrm{d}s_\alpha \int_0^{N_2} \mathrm{d}s_\beta U_{\alpha\beta}[\mathbf{R}_\alpha(s_\alpha)$$

$$-\mathbf{R}_\beta(s_\beta)], \tag{4}$$

and

$$\begin{aligned} U_b = &\sum_{\alpha=1}^{n_1}\int_0^{N_1} \mathrm{d}s_\alpha \sum_{i=1}^{n_s} U_{\alpha s}[\mathbf{R}_\alpha(s_\alpha)-\mathbf{r}_i] \\ &+\sum_{\beta=1}^{n_2}\int_0^{N_2} \mathrm{d}s_\beta \sum_{i=1}^{n_s} U_{\beta s}[\mathbf{R}_\beta(s_\beta)-\mathbf{r}_i] \\ &+\sum_{\alpha=1}^{n_1}\int_0^{N_1} \mathrm{d}s_\alpha \sum_{i=1}^{n_c+\sum_\gamma n_\gamma} U_{\alpha i}[\mathbf{R}_\alpha(s_\alpha)-\mathbf{r}_i] \\ &+\sum_{\beta=1}^{n_2}\int_0^{N_2} \mathrm{d}s_\beta \sum_{i=1}^{n_c+\sum_\gamma n_\gamma} U_{\beta i}[\mathbf{R}_\beta(s_\beta)-\mathbf{r}_i] \\ &+\frac{1}{2}\sum_{i=1}^{n_s}\sum_{j=1}^{n_s} U_{ss}(\mathbf{r}_i-\mathbf{r}_j) \\ &+\frac{1}{2}\sum_{i=1}^{n_c+\sum_\gamma n_\gamma}\sum_{j=1}^{n_c+\sum_\gamma n_\gamma} U_{ij}(\mathbf{r}_i-\mathbf{r}_j). \end{aligned} \tag{5}$$

Here $\mathbf{R}_\alpha(s_\alpha)$ is the position vector of the arc length variable $s_\alpha (0 \le s_\alpha \le N_1)$ of the α-th chain. Similarly, $\mathbf{R}_\beta(s_\beta)$ denotes the arc length position for the β-th chain. $U_{\alpha\alpha'}(\mathbf{r})$ is the interaction energy between two segments of polycations separated by a distance $\mathbf{r}$. Similarly, the pairwise interaction energies for two segments of polyanion chains and for a pair of a polycation segment and a polyanion segment are given by $U_{\beta\beta'}(\mathbf{r})$ and $U_{\alpha\beta}(\mathbf{r})$, respectively,

$$\begin{aligned} U_{\alpha\alpha'}(\mathbf{r}) = w_{11}\ell^3\delta(\mathbf{r}) + \frac{\alpha^2 z_p^2 \ell_B}{r}, U_{\beta\beta'}(\mathbf{r}) = w_{22}\ell^3\delta(\mathbf{r}) \\ + \frac{\alpha^2 z_p^2 \ell_B}{r}, U_{\alpha\beta}(\mathbf{r}) = w_{12}\ell^3\delta(\mathbf{r}) - \frac{\alpha^2 z_p^2 \ell_B}{r}, \end{aligned} \tag{6}$$

where w_{11}, w_{22}, and w_{12} are excluded volume pseudopotentials, which are related to the Flory-Huggins parameters χ_{11}, χ_{22}, and χ_{12}, according to $w_{11} = (1 - 2\chi_{11})\ell^3, w_{22} = (1 - 2\chi_{22})\ell^3$, and $w_{12} = (1 - 2\chi_{12})\ell^3$. $\delta(\mathbf{r})$ is the Dirac delta function and $r = |\mathbf{r}|$. The second terms on the right hand side of Eq. (6) represent the Coulomb interaction energy between the segments, where ℓ_B is the Bjerrum length,

$$\ell_B = \frac{e^2}{4\pi\epsilon_0\epsilon k_B T}. \tag{7}$$

The short-ranged interactions between the polymer segments and solvent molecules ($U_{ps} = U_{\alpha s}, U_{\beta s}$) and between solvent molecules (U_{ss}) are given by

$$U_{ps}(\mathbf{r}) = w_{ps}\delta(\mathbf{r}) \text{ and } U_{ss}(\mathbf{r}) = w_{ss}\delta(\mathbf{r}), \tag{8}$$

where w_{ps} and w_{ss} are the corresponding pseudopotential excluded volume parameters. The electrostatic interactions between charged segments ($p = \alpha, \beta$) and various ions are given by

$$U_{pi}(\mathbf{r}) = \frac{\alpha z_p z_i \ell_B}{r} \qquad \text{and} \qquad U_{ij}(\mathbf{r}) = \frac{z_i z_j \ell_B}{r}. \tag{9}$$

The above set of equations defines the model.

3 General theory

As a first step, all degrees of freedom associated with mobile (dissociated) counterions, electrolyte ions, and solvent molecules are integrated out in Eq. (1). This step is carried out with the Debye–Hückel theory of a charged plasma (here corresponding to the charged solution background which neutralizes the polyelectrolyte charges). As a result, the inter-segment interaction between polymer segments is given by the screened Coulomb potential (in addition to the hydrophobic part) as [3]

$$\begin{aligned} v_{\alpha\alpha'}(\mathbf{r}) &= w_{11}\ell^3\delta(\mathbf{r}) + w_c\frac{e^{-\kappa r}}{4\pi r}, \\ v_{\beta\beta'}(\mathbf{r}) &= w_{22}\ell^3\delta(\mathbf{r}) + w_c\frac{e^{-\kappa r}}{4\pi r}, \\ v_{\alpha\beta}(\mathbf{r}) &= w_{12}\ell^3\delta(\mathbf{r}) - w_c\frac{e^{-\kappa r}}{4\pi r}, \end{aligned} \tag{10}$$

where

$$w_c = 4\pi\alpha^2 z_p^2 \ell_B, \tag{11}$$

and

$$\kappa^2 = \frac{4\pi\ell_B}{V}\left(z_c^2 n_c + \sum_\gamma z_\gamma^2 n_\gamma\right). \tag{12}$$

It should be noted that the above form of the screened Coulomb electrostatic interaction is only within the Debye–Hückel theory. This is valid even when the background medium contains a net charge, due to counterions from nonstoichiometric composition of polycations and polyanions (as in one-component plasma). If the electrolyte concentration is very high, deviations from the Debye–Hückel theory will arise and a treatment of non-linear Poisson-Boltzmann formalism needs to be implemented. Furthermore, the excluded volume interactions among the electrolyte ions, due to their finite size, are also ignored. In the present paper, we consider only the simple Debye–Hückel screening form in the interest of analytical tractability in obtaining physically significant results of experimental relevance.

After the first step, the system consists of only n_1 polycations and n_2 polyanions which are coupled through both intra-chain and inter-chain interaction potential $v(\mathbf{r})$ given by Eq. (10). The Helmholtz free

energy F of the whole system is now given by the free energy F_p of these chains and the free energy of the background F_b as

$$F = F_p + F_b. \tag{13}$$

The free energy of the background fluid consists of the entropy of mixing terms and the charge fluctuations in the neutralizing background,

$$F_b = F_{b0} + F_{fl,i}, \tag{14}$$

where

$$\frac{F_{b0}}{k_BTV} = c_s \ln c_s - c_s + c_{1c} \ln c_{1c} - c_{1c} + c_{2c} \ln c_{2c} - c_{2c} + \sum_\gamma [c_\gamma \ln c_\gamma - c_\gamma] + \frac{1}{2} w_{ss} c_s^2 + w_{ps} c c_s, \tag{15}$$

and

$$\frac{F_{fl,i}}{k_BTV} = -\frac{\kappa^3}{12\pi}. \tag{16}$$

It should be noted that the expression for $F_{fl,i}$ given by Eq. (16) is strictly valid only in the region of validity of the Debye–Hückel theory, namely the local electric potential being less than k_BT. Extensions can be made to go beyond the linearized Poisson-Boltzmann formalism [2]. Extension to include the finite size of the ions generalizes Eq. (16) to

$$\frac{F_{fl,i}}{k_BT} = -\frac{V}{4\pi\ell^3}[\ln(1+\kappa\ell) - \kappa\ell + \frac{1}{2}\kappa^2\ell^2]. \tag{17}$$

The free energy F_p of n_1 polycations and n_2 polyanions in the background, where the interaction energy between any two segments separated by distance r is given by Eq. (10), follows from Eq. (1) as

$$e^{-\frac{F_p}{k_BT}} = \frac{1}{n_1! n_2!} \int \prod_{\alpha=1}^{n_1} \mathcal{D}[\mathbf{R}_\alpha] \int \prod_{\beta=1}^{n_2} \mathcal{D}[\mathbf{R}_\beta] \exp\left[-\mathcal{L}_\alpha - \mathcal{L}_\beta - v\right], \tag{18}$$

where

$$v = \frac{1}{2}\sum_{\alpha=1}^{n_1}\sum_{\alpha'=1}^{n_1}\int_0^{N_1} \mathrm{d}s_\alpha \int_0^{N_1} \mathrm{d}s_{\alpha'} v_{\alpha\alpha'}[\mathbf{R}_\alpha(s_\alpha) - \mathbf{R}_{\alpha'}(s_{\alpha'})] + \frac{1}{2}\sum_{\beta=1}^{n_2}\sum_{\beta'=1}^{n_2}\int_0^{N_2} \mathrm{d}s_\beta \int_0^{N_2} \mathrm{d}s_{\beta'} v_{\beta\beta'}[\mathbf{R}_\beta(s_\beta) - \mathbf{R}_{\beta'}(s_{\beta'})] + \sum_{\alpha=1}^{n_1}\sum_{\beta=1}^{n_2}\int_0^{N_1} \mathrm{d}s_\alpha \int_0^{N_2} \mathrm{d}s_\beta v_{\alpha\beta}[\mathbf{R}_\alpha(s_\alpha) - \mathbf{R}_\beta(s_\beta)]. \tag{19}$$

Let us introduce two collective coordinates as the local monomer concentrations of the polycations and polyanions. Defining the local monomer concentration $c_1(\mathbf{r})$ of polycations as

$$c_1(\mathbf{r}) = \sum_{\alpha=1}^{n_1}\int_0^{N_1} \mathrm{d}s_\alpha \delta(\mathbf{r} - \mathbf{R}_\alpha(s_\alpha)) \tag{20}$$

and its Fourier transform as

$$c_{1,\mathbf{k}} = \frac{1}{V}\int \mathrm{d}\mathbf{r} e^{i\mathbf{k}\cdot\mathbf{r}} c_1(\mathbf{r}) = \frac{1}{V}\sum_{\alpha=1}^{n_1} \int_0^{N_1} \mathrm{d}s_\alpha e^{i\mathbf{k}\cdot\mathbf{R}_\alpha(s_\alpha)}, \tag{21}$$

so that the relation between $c_1(\mathbf{r})$ and $c_{1,\mathbf{k}}$ is

$$c_1(\mathbf{r}) = V\int \frac{d^3k}{(2\pi)^3} c_{1,\mathbf{k}} e^{-i\mathbf{k}\cdot\mathbf{r}} = \sum_{\mathbf{k}} c_{1,\mathbf{k}} e^{-i\mathbf{k}\cdot\mathbf{r}}. \tag{22}$$

Similarly, the local monomer concentration of polyanion and its Fourier transform are related as

$$c_2(\mathbf{r}) = \sum_{\beta=1}^{n_2}\int_0^{N_2} \mathrm{d}s_\beta \delta(\mathbf{r} - \mathbf{R}_\beta(s_\beta)) = V\int \frac{d^3k}{(2\pi)^3} c_{2,\mathbf{k}} e^{-i\mathbf{k}\cdot\mathbf{r}} = \sum_{\mathbf{k}} c_{2,\mathbf{k}} e^{-i\mathbf{k}\cdot\mathbf{r}} \tag{23}$$

and

$$c_{2,\mathbf{k}} = \frac{1}{V}\int \mathrm{d}\mathbf{r} e^{i\mathbf{k}\cdot\mathbf{r}} c_2(\mathbf{r}) = \frac{1}{V}\sum_{\beta=1}^{n_2}\int_0^{N_2} \mathrm{d}s_\beta e^{i\mathbf{k}\cdot\mathbf{R}_\beta(s_\beta)}, \tag{24}$$

Using Eq. (10) and the Fourier transform of $v_{\alpha\alpha'}(\mathbf{r})$ defined below, we get

$$v_{\alpha\alpha'}[\mathbf{R}_\alpha(s_\alpha) - \mathbf{R}_{\alpha'}(s_{\alpha'})] = \int \frac{d^3k}{(2\pi)^3}\left(w_{11}\ell^3 + v_k\right) e^{-i\mathbf{k}\cdot[\mathbf{R}_\alpha(s_\alpha) - \mathbf{R}_{\alpha'}(s_{\alpha'})]}, \tag{25}$$

where

$$v_k = \frac{4\pi\alpha^2 z_p^2 \ell_B}{k^2+\kappa^2} \equiv \frac{w_c}{k^2+\kappa^2}. \tag{26}$$

Using Equations (21) and (25), the first term on the right-hand-side of Eq. (19) becomes

$$\begin{aligned}&\frac{1}{2}\sum_{\alpha=1}^{n_1}\sum_{\alpha'=1}^{n_1}\int_0^{N_1}\mathrm{d}s_\alpha\int_0^{N_1}\mathrm{d}s'_\alpha v_{\alpha\alpha'}[\mathbf{R}_\alpha(s_\alpha)-\mathbf{R}_{\alpha'}(s'_\alpha)]\\&=\frac{V^2}{2}\int\frac{d^3k}{(2\pi)^3}\left(w_{11}\ell^3+v_k\right)c_{1,\mathbf{k}}c_{1,-\mathbf{k}}\\&=\frac{V}{2}\sum_{\mathbf{k}}\left(w_{11}\ell^3+v_k\right)c_{1,\mathbf{k}}c_{1,-\mathbf{k}}.\end{aligned}\tag{27}$$

Similarly, the other two terms on the right-hand-side of Eq. (19) are given by

$$\begin{aligned}&\frac{1}{2}\sum_{\beta=1}^{n_2}\sum_{\beta'=1}^{n_2}\int_0^{N_2}\mathrm{d}s_\beta\int_0^{N_2}\mathrm{d}s'_\beta v_{\beta\beta'}[\mathbf{R}_\beta(s_\beta)-\mathbf{R}_{\beta'}(s'_\beta)]\\&=\frac{V}{2}\sum_{\mathbf{k}}\left(w_{22}\ell^3+v_k\right)c_{2,\mathbf{k}}c_{2,-\mathbf{k}},\end{aligned}\tag{28}$$

$$\begin{aligned}&\sum_{\alpha=1}^{n_1}\sum_{\beta=1}^{n_2}\int_0^{N_1}\mathrm{d}s_\alpha\int_0^{N_2}\mathrm{d}s_\beta v_{\alpha\beta}[\mathbf{R}_\alpha(s_\alpha)-\mathbf{R}_\beta(s_\beta)]\\&=V\sum_{\mathbf{k}}\left(w_{12}\ell^3+v_k\right)c_{1,\mathbf{k}}c_{2,-\mathbf{k}}.\end{aligned}\tag{29}$$

Using the collective coordinates $c_{1,\mathbf{k}}$ and $c_{2,\mathbf{k}}$, the free energy term U from the segment-segment interactions given by Eq. (4) becomes

$$U=U_{\text{excluded-volume}}+U_{\text{electrostatic}},\tag{30}$$

where

$$\begin{aligned}U_{\text{excluded-volume}}=\frac{V\ell^3}{2}\sum_{\mathbf{k}}[&w_{11}c_{1,\mathbf{k}}c_{1,-\mathbf{k}}\\&+w_{22}c_{2,\mathbf{k}}c_{2,-\mathbf{k}}+2w_{12}c_{1,\mathbf{k}}c_{2,-\mathbf{k}}]\end{aligned}\tag{31}$$

and

$$U_{\text{electrostatic}}=\frac{V}{2}\sum_{\mathbf{k}}v_k\left(c_{1,\mathbf{k}}-c_{2,\mathbf{k}}\right)^2.\tag{32}$$

Note that not all $c_{1,\mathbf{k}}$ are independent since $c_{1,-\mathbf{k}}=c^\star_{1,\mathbf{k}}$. Therefore, we choose $c_{1,\mathbf{k}}$ with $\mathbf{k}>0$ as independent components representing all fluctuations. The $\mathbf{k}=0$ component is obviously the mean field component given as

$$c_{1,\mathbf{k}=0}=\frac{n_1N_1}{V}=c_1^0\text{and }c_{2,\mathbf{k}=0}=\frac{n_2N_2}{V}=c_2^0,\tag{33}$$

where c_1^0 and c_2^0 are the average monomer concentrations of the polycation and polyanion, respectively.

4 Mean field theory

Using the incompressibility constraint, and ignoring the constant terms linear in c_1^0 and c_2^0, the mean field part of $U_{\text{excluded-volume}}$ follows from Eqs. (31) and (34) as

$$U_{\text{excluded-volume}}=V\ell^3\chi c_1^0c_2^0,\tag{34}$$

where χ is the Flory-Huggins parameter denoting the chemical mismatch among the backbones of polycation and polyanion and solvent,

$$\chi=\left[w_{12}-\frac{1}{2}\left(w_{11}+w_{22}\right)\right].\tag{35}$$

The mean field contribution to the electrostatic free energy $U_{\text{electrostatic}}$ follows from Eqs. (32) and (33) as

$$U_{\text{electrostatic}}=\frac{V}{2}v_0\left(c_1^0-c_2^0\right),\tag{36}$$

where v_0 is w_c/κ^2. Hence, for the symmetric case $c_1^0=c_2^0$, the mean field part of $U_{\text{electrostatic}}$ is zero,

$$U_{\text{electrostatic}}=0.\tag{37}$$

Thus at the mean field level, there is no electrostatic contribution to the conformation of individual chains and thermodynamics in a symmetric coacervate system, and the system follows the behavior of the corresponding uncharged system. For example, in the absence of excluded volume interactions, the chains obey Gaussian chain statistics with the size exponent $\nu=1/2$.

5 Fluctuations

In order to treat concentration fluctuations in the system, let us define the non-local order parameter $\psi(\mathbf{r})$ in terms of the local concentrations of polycation and polyanion as

$$\psi(\mathbf{r})=\frac{1}{2}\left[c_1(\mathbf{r})-c_2(\mathbf{r})\right],\tag{38}$$

with the constraint

$$c_1(\mathbf{r})+c_2(\mathbf{r})=c_0,\tag{39}$$

where c_0 is the average total polymer concentration. Introducing these constraints, the polymer contribution to the free energy F_p follows from Eq. (18) as

$$\begin{aligned}e^{-\frac{F_p}{k_BT}}=\frac{1}{n_1!n_2!}\int\delta\psi\int\prod_{\alpha=1}^{n_1}\mathcal{D}[\mathbf{R}_\alpha]\\\int\prod_{\beta=1}^{n_2}\mathcal{D}[\mathbf{R}_\beta]\exp\left[-\mathcal{L}_\alpha-\mathcal{L}_\beta-v\right]\end{aligned}$$

$$\times \prod_{\mathbf{r}} \delta\left[2\psi(\mathbf{r}) - c_1(\mathbf{r}) + c_2(\mathbf{r})\right] \prod_{\mathbf{r}} \delta\left[c_1(\mathbf{r}) + c_2(\mathbf{r}) - c_0\right]. \quad (40)$$

Expressing $c_1(\mathbf{r}), c_2(\mathbf{r})$, and $\psi(\mathbf{r})$ in terms of their corresponding Fourier transforms $c_{1,\mathbf{k}}, c_{2.\mathbf{k}}$, and $\psi_{\mathbf{k}}$, we get [2–4]

$$e^{-\frac{F_p}{k_B T}} = \int \prod_{\mathbf{k}>0} \delta\psi_{\mathbf{k}} \exp\left[-\frac{V}{2}\sum_{\mathbf{k}} \left(-2\chi\ell^3 + 4v_k\right)\psi_{\mathbf{k}}\psi_{-\mathbf{k}}\right] \times \int \prod_{\mathbf{k}>0} \frac{d\phi_{\mathbf{k}}}{\pi^2} \int \prod_{\mathbf{k}>0} \frac{d\phi'_{\mathbf{k}}}{\pi^2} \int \prod_{\alpha=1}^{n_1} \mathcal{D}[\mathbf{R}_\alpha] \int \prod_{\beta=1}^{n_2} \mathcal{D}[\mathbf{R}_\beta] \exp\left[-\mathcal{L}_\alpha - \mathcal{L}_\beta\right] \times \exp\left[i\sum_{\mathbf{k}\neq 0} \theta_{\mathbf{k}}\phi_{-\mathbf{k}} + i\sum_{\mathbf{k}\neq 0} \theta'_{\mathbf{k}}\phi'_{-\mathbf{k}}\right], \quad (41)$$

where $\phi_{-\mathbf{k}}$ and $\phi'_{-\mathbf{k}}$ are field variables as described in detail in Refs.2-4, and

$$\theta_{\mathbf{k}} = 2\psi_{\mathbf{k}} - \frac{1}{V}\sum_{\alpha=1}^{n_1} \int_0^{N_1} \mathrm{d}s_\alpha e^{i\mathbf{k}\cdot\mathbf{R}_\alpha(s_\alpha)} + \frac{1}{V}\sum_{\beta=1}^{n_2} \int_0^{N_2} \mathrm{d}s_\beta e^{i\mathbf{k}\cdot\mathbf{R}_\beta(s_\beta)}, \quad (42)$$

and

$$\theta'_{\mathbf{k}} = \frac{1}{V}\sum_{\alpha=1}^{n_1} \int_0^{N_1} \mathrm{d}s_\alpha e^{i\mathbf{k}\cdot\mathbf{R}_\alpha(s_\alpha)} + \frac{1}{V}\sum_{\beta=1}^{n_2} \int_0^{N_2} \mathrm{d}s_\beta e^{i\mathbf{k}\cdot\mathbf{R}_\beta(s_\beta)} - c_0. \quad (43)$$

The $\mathbf{k} = 0$ contribution in Eq. (40) carries the translational entropy of the chains. Performing the integrals over polymer conformations, Eqs. (41)–(43) yield within the random phase approximation,

$$\int \prod_{\alpha=1}^{n_1} \mathcal{D}[\mathbf{R}_\alpha] \int \prod_{\beta=1}^{n_2} \mathcal{D}[\mathbf{R}_\beta] \exp\left[-\mathcal{L}_\alpha - \mathcal{L}_\beta + i\sum_{\mathbf{k}\neq 0} \theta_{\mathbf{k}}\phi_{-\mathbf{k}} + \sum_{\mathbf{k}\neq 0} \theta'_{\mathbf{k}}\phi'_{-\mathbf{k}}\right] = \exp\left[2i\sum_{\mathbf{k}\neq 0} \psi_{\mathbf{k}}\phi_{-\mathbf{k}} - \frac{1}{2V}\sum_{\mathbf{k}\neq 0} \phi_{\mathbf{k}}\left(S_1(k) + S_2(k)\right)\phi_{-\mathbf{k}}\right] \times \exp\left[-\frac{1}{2V}\sum_{\mathbf{k}\neq 0} \phi'_{\mathbf{k}}\left(S_1(k) + S_2(k)\right)\phi'_{-\mathbf{k}} + \frac{1}{V}\sum_{\mathbf{k}\neq 0} \phi_{\mathbf{k}}\left(S_1(k) - S_2(k)\right)\phi'_{-\mathbf{k}}\right], \quad (44)$$

where $S_1(k)$ is given by

$$S_1(k) = \frac{n_1 N_1}{V} S_{D1}(k), \quad (45)$$

with $S_{D1}(k)$ being the Debye structure factor for the polycation (polymer component 1)

$$S_{D1}(k) = \frac{2N_1}{k^4 R_{g1}^4}\left(e^{-k^2 R_{g1}^2} - 1 + k^2 R_{g1}^2\right), \quad (46)$$

where R_{g1} is the radius of gyration of a Gaussian chain with N_1 Kuhn segments each of segment length ℓ ($R_{g1}^2 = N_1\ell^2/6$). Since $n_1 N_1/V = c_1^0 = \phi_1/\ell^3$, where ϕ_1 is the volume fraction of the polycation, Eqs. (45) and (46) give

$$S_1(k) = \frac{\phi_1}{\ell^3}\frac{2N_1}{k^4 R_{g1}^4}\left(e^{-k^2 R_{g1}^2} - 1 + k^2 R_{g1}^2\right), \quad (47)$$

Similarly, $S_2(k)$ is defined for the polyanion (second component) by replacing the subscript 1 in Eqs. (45)–(47) by 2.

Now, performing the integrations $\int \prod_{\mathbf{k}>0} \frac{d\phi_{\mathbf{k}}}{\pi^2} \int \prod_{\mathbf{k}>0} \frac{d\phi'_{\mathbf{k}}}{\pi^2}$ in Eq. (41) over the argument given by Eq. (44), we get

$$\frac{\pi V}{\sqrt{S_1(k)S_2(k)}} e^{-\frac{V}{2}\sum_{\mathbf{k}\neq 0}\left(\frac{1}{S_1(k)} + \frac{1}{S_2(k)}\right)\psi_{\mathbf{k}}\psi_{-\mathbf{k}}} \quad (48)$$

Substituting this result in Eq. (41) yields

$$e^{-\frac{F_p}{k_B T}} = \int \prod_{\mathbf{k}>0} \delta\psi_{\mathbf{k}} \exp\left[-\frac{V}{2}\sum_{\mathbf{k}\neq 0}\left(\frac{1}{S_1(k)} + \frac{1}{S_2(k)} - 2\chi\ell^3 + 4v_k\right)\psi_{\mathbf{k}}\psi_{-\mathbf{k}}\right], \quad (49)$$

where the pre-exponential factor in Expression (48) is ignored. The two-point correlation function of the fluctuation $\psi_{\mathbf{k}}$ follows from the Gaussian distribution given by Eq. (49) as

$$\langle\psi_{\mathbf{k}}\psi_{-\mathbf{k}}\rangle = \frac{1}{V\left[\frac{1}{S_1(k)} + \frac{1}{S_2(k)} - 2\chi\ell^3 + 4v_k\right]}. \quad (50)$$

Using the above equations, we present below results on the scattered intensity $I(k)$ which is proportional to

$\langle\psi_{\mathbf{k}}\psi_{-\mathbf{k}}\rangle$ in the four regimes ($kR_g<1, kR_g>1, k\xi_D<1$, $k\xi_D>1$) described in Fig. 1b. This result is a generalization of the classical Ornstein–Zernike form for the two-point correlation function of concentration fluctuations.

V.1. Regime 1 ($kR_g \ll 1$,high salt):

Expanding $S_1(k)$ given by Eq. (47) in the limit of $kR_g \ll 1$, we get

$$\frac{1}{S_1(k)} = \frac{\ell^3}{\phi_1 N_1}\left(1+\frac{k^2 N_1 \ell^2}{18}+\cdots\right) = \ell^3\left[\frac{1}{\phi_1 N_1}+\frac{1}{18}\frac{k^2\ell^2}{\phi_1}+\cdots\right]. \quad (51)$$

Similarly, $1/S_2(k)$ is given by

$$\frac{1}{S_2(k)} = \frac{\ell^3}{\phi_2 N_2}\left(1+\frac{k^2 N_2 \ell^2}{18}+\cdots\right) = \ell^3\left[\frac{1}{\phi_1 N_2}+\frac{1}{18}\frac{k^2\ell^2}{\phi_2}+\cdots\right]. \quad (52)$$

Substituting Eqs. (51) and (52) in Eq. (50), we get

$$\langle\psi_{\mathbf{k}}\psi_{-\mathbf{k}}\rangle = \frac{1}{V\ell^3}\frac{1}{\left[\left(\frac{1}{\phi_1 N_1}+\frac{1}{\phi_2 N_2}-2\chi+4\frac{v_k}{\ell^3}\right)+\frac{k^2\ell^2}{18}\left(\frac{1}{\phi_1}+\frac{1}{\phi_2}\right)\right]} \quad (53)$$

Since the total polymer volume fraction ϕ_0 is $\phi_1+\phi_2$, we get

$$\langle\psi_{\mathbf{k}}\psi_{-\mathbf{k}}\rangle = \frac{1}{V\ell^3}\frac{1}{\left[\left(\frac{1}{\phi_1 N_1}+\frac{1}{\phi_2 N_2}+4\frac{v_k}{\ell^3}-2\chi\right)+\frac{\phi_0}{18\phi_1\phi_2}k^2\ell^2\right]} \quad (54)$$

This result can be rewritten as

$$\langle\psi_{\mathbf{k}}\psi_{-\mathbf{k}}\rangle = \frac{1}{V\ell^3}\frac{1}{\left[2(\chi_s-\chi)+\frac{\phi_0}{18\phi_1\phi_2}k^2\ell^2\right]}, \quad (55)$$

where the spinodal chi (χ_s) is

$$\chi_s = \frac{1}{2}\left[\frac{1}{\phi_1 N_1}+\frac{1}{\phi_2 N_2}+4\frac{v_k}{\ell^3}\right]. \quad (56)$$

In the high salt limit ($\kappa^2 \gg k^2$), v_k of Eq. (26) is given by

$$\frac{v_k}{\ell^3} = \frac{w_c}{\ell}\frac{1}{\kappa^2\ell^2}. \quad (57)$$

Substituting this result in Eq. (56), χ_s becomes

$$\chi_s = \frac{1}{2}\left[\frac{1}{\phi_1 N_1}+\frac{1}{\phi_2 N_2}+\frac{4w_c}{\kappa^2\ell^3}\right] = \frac{1}{2}\left(\frac{1}{\phi_1 N_1}+\frac{1}{\phi_2 N_2}\right)+\frac{8\pi\alpha^2 z_p^2\ell_B}{\kappa^2\ell^3}. \quad (58)$$

Thus, the spinodal chi is shifted up by the electrostatic interactions as given by this equation. Combining Eqs. (55)–(58), we get the structure factor for the concentration fluctuations as

$$\langle\psi_{\mathbf{k}}\psi_{-\mathbf{k}}\rangle = \frac{1}{V\ell^3}\frac{1}{\left[2(\chi_s-\chi)(1+k^2\xi^2)\right]}, \quad (59)$$

where the correlation length ξ for the concentration fluctuations is given by

$$\left(\frac{\xi}{\ell}\right)^2 = \frac{\phi_0}{36\phi_1\phi_2(\chi_s-\chi)}. \quad (60)$$

Equation (59) is in the Ornstein–Zernike form for the scattering intensity exhibiting a monotonic decrease in scattering intensity with scattering wave vector (sketched in Fig. 3a).The inverse scattering intensity follows as

$$\frac{1}{I(k)} \sim \frac{1}{\langle\psi_{\mathbf{k}}\psi_{-\mathbf{k}}\rangle} \sim 2(\chi_s-\chi)\left(1+k^2\xi^2\right). \quad (61)$$

Therefore, the scattering intensity extrapolated at zero wave vector diverges as in the mean field theory of critical phenomena in three-dimensional Ising systems as

$$I(k\to 0) \sim \frac{1}{(\chi_s-\chi)^\gamma} \sim \frac{1}{|T-T_s|^\gamma}, \quad \gamma = 1 \quad (62)$$

where γ is the susceptibility critical exponent and upper critical solution behavior is assumed in connecting temperature with χ. The shift in the spinodal temperature due to electrostatic interaction is given by Eq. (58). Analogously, the correlation length ξ of Eq. (60) diverges as in the mean field theory upon approach towards the spinodal condition as given by

$$\xi \sim \frac{1}{(\chi_s-\chi)^\nu} \sim \frac{1}{|T-T_s|^\nu}, \qquad \nu = \frac{1}{2}. \quad (63)$$

Combining Eqs. (49), (55), and (58), the free energy functional $F[\psi]$ is of the Landau–Ginzburg form,

$$\frac{F[\psi]}{k_B T} = \frac{V\ell^3}{2}\sum_{\mathbf{k}\neq 0}\left[\left(\frac{1}{\phi_1 N_1}+\frac{1}{\phi_2 N_2}+\frac{16\pi\alpha^2 z_p^2\ell_B}{\kappa^2\ell^3}-2\chi\right)+\frac{\phi_0 k^2\ell^2}{18\phi_1\phi_2}\right]\psi_{\mathbf{k}}\psi_{-\mathbf{k}}. \quad (64)$$

This expression is useful in predicting phase diagrams at high enough salt concentrations in the solution.

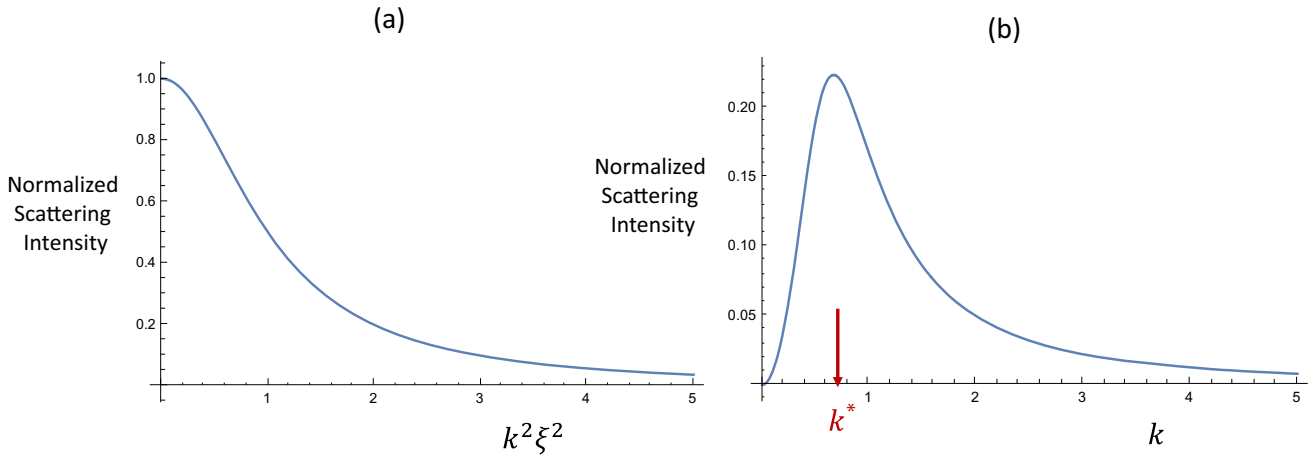

Fig. 3 **a** Sketch of the Ornstein–Zernike behavior of the monotonic dependence of scattering intensity on the scattering wave vector, to be observed at higher salt concentration. **b** Emergence of a scattering peak at lower salt concentrations

V.2. Regime 2 ($kR_g \ll 1$,no salt):
In the low salt limit, $\kappa \to 0$, v_k of Eq. (26) is given by

$$\frac{v_k}{\ell^3} = \frac{w_c}{\ell}\frac{1}{k^2\ell^2}. \tag{65}$$

Therefore, Eqs. (49) and (54) give

$$\langle \psi_{\mathbf{k}}\psi_{-\mathbf{k}}\rangle = \frac{1}{V\ell^3}\frac{1}{\left[\left(\frac{1}{\phi_1 N_1}+\frac{1}{\phi_2 N_2}+\frac{4w_c}{k^2\ell^3}-2\chi\right)+\frac{\phi_0}{18\phi_1\phi_2}k^2\ell^2\right]}, \tag{66}$$

and the free energy functional as

$$\frac{F[\psi]}{k_BT} = \frac{V\ell^3}{2}\sum_{\mathbf{k}\neq 0}\left[\left(\frac{1}{\phi_1 N_1}+\frac{1}{\phi_2 N_2}+\frac{4w_c}{k^2\ell^3}-2\chi\right)+\frac{\phi_0 k^2\ell^2}{18\phi_1\phi_2}\right]\psi_{\mathbf{k}}\psi_{-\mathbf{k}}, \tag{67}$$

which is in the Landau–Ginzburg–Brazovskii form. Rewriting Eq. (66), we get

$$\langle \psi_{\mathbf{k}}\psi_{-\mathbf{k}}\rangle = \frac{1}{V\ell^3}\frac{k^2\ell^2}{\left[\frac{4w_c}{\ell}+\left(\frac{1}{\phi_1 N_1}+\frac{1}{\phi_2 N_2}-2\chi\right)k^2\ell^2+\frac{\phi_0}{18\phi_1\phi_2}k^4\ell^4\right]} \tag{68}$$

This exhibits a peak at the scattering wave vector $k^\star$, as would be seen in scattering intensity (sketched in Fig. 3b), given by

$$k^\star\ell = \left(\frac{72w_c\phi_1\phi_2}{\phi_0\ell}\right)^{1/4} = \left(\frac{288\alpha^2 z_p^2\ell_B\phi_1\phi_2}{\phi_0\ell}\right)^{1/4} \tag{69}$$

where Eq. (26) has been used.

V.3. Regime 3 ($kR_g \gg 1$,high salt):
In the limit of $kR_g \gg 1$, $S_{D1}(k)$ of Eq. (46) becomes

$$S_{D1}(k) = \frac{12}{k^2\ell^2}, \tag{70}$$

so that S_1 of Eq. (45) is given by

$$S_1(k) = \frac{n_1N_1}{V}S_{D1}(k) = c_1^0 S_{D1}(k) = \frac{\phi_1}{\ell^3}S_{D1}(k) = \frac{\phi_1}{\ell^3}\frac{12}{k^2\ell^2}. \tag{71}$$

Substituting this result and the analogous expression for $S_2(k)$ in Eq. (50), we get

$$\langle \psi_{\mathbf{k}}\psi_{-\mathbf{k}}\rangle = \frac{1}{V\left[\frac{k^2\ell^2}{12}\frac{\ell^3}{\phi_1}+\frac{k^2\ell^2}{12}\frac{\ell^3}{\phi_2}-2\chi\ell^3+4v_k\right]}. \tag{72}$$

Using $\phi_1+\phi_2=\phi_0$ (total polymer concentration), this equation becomes

$$\langle \psi_{\mathbf{k}}\psi_{-\mathbf{k}}\rangle = \frac{12}{V\ell^5}\frac{\phi_1\phi_2}{\phi_0}\frac{1}{\left[k^2+\frac{12}{\ell^2}\frac{\phi_1\phi_2}{\phi_0}\left(-2\chi+\frac{4v_k}{\ell^3}\right)\right]}. \tag{73}$$

In the high salt limit, $\kappa \gg k$, and using Eq. (57), the scattering intensity is proportional to

$$\langle \psi_{\mathbf{k}}\psi_{-\mathbf{k}}\rangle = \frac{12}{V\ell^5}\frac{\phi_1\phi_2}{\phi_0}\frac{1}{\left[k^2+\frac{12}{\ell^2}\frac{\phi_1\phi_2}{\phi_0}\left(-2\chi+\frac{4w_c}{\kappa^2\ell^3}\right)\right]}. \tag{74}$$

Again, in this regime, the correlation function is of the Ornstein–Zernike form (sketched in Fig. 3a) with the

correlation length ξ given by

$$\xi^{-2} = \frac{12}{\ell^2}\frac{\phi_1\phi_2}{\phi_0}\left(-2\chi + \frac{4w_c}{\kappa^2\ell^3}\right). \tag{75}$$

If electrostatic interactions dominate over the short-ranged excluded volume interactions, the correlation length is given by

$$\xi^{-2} = \frac{48}{\ell^2}\frac{\phi_1\phi_2}{\phi_0}\frac{w_c}{\kappa^2\ell^3} = \frac{192\pi}{\ell^2}\frac{\phi_1\phi_2}{\phi_0}\frac{\alpha^2 z_p^2\ell_B}{\kappa^2\ell^3} \tag{76}$$

This result is independent of N_1 and N_2 in comparison with Eq. (60) valid for small scattering angles.

V.4. Regime 4 ($kR_g \gg 1$,no salt):
In the low salt limit, $\kappa \to 0$, v_k is given by Eq. (65). Therefore, Eq. (74) gives

$$\langle\psi_{\mathbf{k}}\psi_{-\mathbf{k}}\rangle = \frac{12}{V\ell^5}\frac{\phi_1\phi_2}{\phi_0}\frac{1}{\left[k^2 + \frac{12}{\ell^2}\frac{\phi_1\phi_2}{\phi_0}\left(-2\chi + \frac{4w_c}{k^2\ell^3}\right)\right]}. \tag{77}$$

Rearranging this equation we get

$$\langle\psi_{\mathbf{k}}\psi_{-\mathbf{k}}\rangle = \frac{1}{V\ell^3}\frac{12}{\ell^2}\frac{\phi_1\phi_2}{\phi_0}\frac{k^2}{\left[k^4 + \frac{12}{\ell^2}\frac{\phi_1\phi_2}{\phi_0}\left(-2\chi + \frac{4w_c}{\ell^3}\right)\right]} \tag{78}$$

This is in the form of the Landau–Ginzburg–Brazovskii correlation function exhibiting a peak in the scattered intensity as sketched in Fig. 3b. The scattering wave vector $k^\star$ at the peak position follows from $\partial\langle\psi_{\mathbf{k}}\psi_{-\mathbf{k}}\rangle/\partial k = 0$ of this equation as

$$k^\star\ell = \left(\frac{48w_c\phi_1\phi_2}{\phi_0\ell}\right)^{1/4} = \left(\frac{192\alpha^2 z_p^2\ell_B\phi_1\phi_2}{\phi_0\ell}\right)^{1/4} \tag{79}$$

The value of the peak position in this regime is $(2/3)^{1/4}$ times the corresponding value in regime 2 given by Eq. (69).

6 Effective inter-segment interaction

Consider a situation where a labelled polycation chain ($\{\mathbf{R}(s)\}$) of the same kind as that in the coacervate is added to a concentrated coacervate of large numbers of polycations and polyanions. Furthermore, let us assume that the electrostatic interaction dominates over the excluded volume interaction. The role of excluded volume has already been discussed in previous publications [5,7,8] and the corresponding result can be simply added to the final formulas derived below. The total free energy of the system $F_{\rm tot}$ is written as

$$\begin{aligned}\frac{F_{\rm tot}}{k_BT} &= \frac{1}{k_BT}F(\{c_1(\mathbf{r}), c_2(\mathbf{r}\}) + \frac{3}{2\ell^2}\int_0^{N_1}\mathrm{d}s\left(\frac{\partial\mathbf{R}(s)}{\partial s}\right)^2\\ &+\frac{1}{2}\int_0^{N_1}\mathrm{d}s\int_0^{N_1}\mathrm{d}s'\frac{1}{V}\sum_{\mathbf{k}}v_k e^{-i\mathbf{k}\cdot[\mathbf{R}(s)-\mathbf{R}(s')]}\\ &+\int_0^{N_1}\mathrm{d}s\sum_{\alpha=1}^{n_1}\int_0^{N_1}\mathrm{d}s_\alpha\frac{1}{V}\sum_{\mathbf{k}}v_k e^{-i\mathbf{k}\cdot[\mathbf{R}(s)-\mathbf{R}_\alpha(s_\alpha)]}\\ &-\int_0^{N_1}\mathrm{d}s\sum_{\beta=1}^{n_2}\int_0^{N_2}\mathrm{d}s_\beta\frac{1}{V}\sum_{\mathbf{k}}v_k e^{-i\mathbf{k}\cdot[\mathbf{R}(s)-\mathbf{R}_\beta(s_\beta)]}\end{aligned} \tag{80}$$

The first term on the right-hand-side of this equation is the free energy of the coacervate before adding the labelled polycation chain. The second term denotes chain connectivity. The rest of the terms correspond to self-interaction, interaction with other polycations, and interactions with all polyanions in the system.

In view of Eqs. (21), (24), and (38), we get

$$\begin{aligned}\frac{F_{\rm tot}}{k_BT} &= \frac{F(\{\psi_{\mathbf{k}}\})}{k_BT} + \frac{3}{2\ell^2}\int_0^{N_1}\mathrm{d}s\left(\frac{\partial\mathbf{R}(s)}{\partial s}\right)^2\\ &+\frac{1}{2}\int_0^{N_1}\mathrm{d}s\int_0^{N_1}\mathrm{d}s'\frac{1}{V}\sum_{\mathbf{k}}v_k e^{-i\mathbf{k}\cdot[\mathbf{R}(s)-\mathbf{R}(s')]}\\ &+2\int_0^{N_1}\mathrm{d}s\sum_{\mathbf{k}}v_k\psi_{\mathbf{k}}e^{-i\mathbf{k}\cdot\mathbf{R}(s)},\end{aligned} \tag{81}$$

where the first term is the free energy of the coacervate expressed in terms of $\psi_{\mathbf{k}}$ as

$$\frac{F(\{\psi_{\mathbf{k}}\})}{k_BT} = \frac{1}{2}\sum_{\mathbf{k}\neq0}\frac{\psi_{\mathbf{k}}\psi_{-\mathbf{k}}}{\langle\psi_{\mathbf{k}}\psi_{-\mathbf{k}}\rangle} \equiv \frac{V}{2}\sum_{\mathbf{k}\neq0}\frac{\psi_{\mathbf{k}}\psi_{-\mathbf{k}}}{g(k)}, \tag{82}$$

with $g(k) = V\langle\psi_{\mathbf{k}}\psi_{-\mathbf{k}}\rangle$.

Integrating over fluctuations,

$$\begin{aligned}\int\prod_{\mathbf{k}>0}\delta\psi_{\mathbf{k}}e^{-\frac{F_{\rm tot}}{k_BT}} &= \exp\left[-\frac{3}{2\ell^2}\int_0^{N_1}\mathrm{d}s\left(\frac{\partial\mathbf{R}(s)}{\partial s}\right)^2\right.\\ &\left.-\frac{1}{2}\int_0^{N_1}\mathrm{d}s\int_0^{N_1}\mathrm{d}s'\frac{1}{V}\sum_{\mathbf{k}}v_k e^{-i\mathbf{k}\cdot[\mathbf{R}(s)-\mathbf{R}(s')]}\right]\\ &\times\int\prod_{\mathbf{k}>0}\delta\psi_{\mathbf{k}}\exp\left[-\frac{V}{2}\sum_{\mathbf{k}\neq0}\frac{\psi_{\mathbf{k}}\psi_{-\mathbf{k}}}{g(k)}\right.\\ &\left.-2\int_0^{N_1}\mathrm{d}s\sum_{\mathbf{k}}v_k\psi_{\mathbf{k}}e^{-i\mathbf{k}\cdot\mathbf{R}(s)}\right].\end{aligned} \tag{83}$$

Performing the integration over $\delta\psi_{\mathbf{k}}$, we get

$$\int\prod_{\mathbf{k}>0}\delta\psi_{\mathbf{k}}\exp\left[-\frac{V}{2}\sum_{\mathbf{k}\neq0}\frac{\psi_{\mathbf{k}}\psi_{-\mathbf{k}}}{g(k)}\right.$$

$$-2\int_0^{N_1} \mathrm{d}s \sum_{\mathbf{k}} v_k \psi_{\mathbf{k}} e^{-i\mathbf{k}\cdot\mathbf{R}(s)}\Bigg] = \prod_{\mathbf{k}>0}\left(\frac{\pi g(k)}{V}\right) \exp\left[\sum_{\mathbf{k}>0}\frac{g(k)}{V} \int_0^{N_1}\mathrm{d}s\int_0^{N_1}\mathrm{d}s'(4v_k^2)e^{-i\mathbf{k}\cdot\left[\mathbf{R}(s)-\mathbf{R}(s')\right]}\right]. \quad (84)$$

Substituting this result in Eq. (83), we obtain

$$\int \prod_{\mathbf{k}>0}\delta\psi_{\mathbf{k}} e^{-\frac{F_{\mathrm{tot}}}{k_BT}} = \prod_{\mathbf{k}>0}\left(\frac{\pi g(k)}{V}\right) \times \exp\left[-\frac{3}{2\ell^2}\int_0^{N_1}\mathrm{d}s\left(\frac{\partial\mathbf{R}(s)}{\partial s}\right)^2 -\frac{1}{V}\int_0^{N_1}\mathrm{d}s\int_0^{N_1}\mathrm{d}s'\sum_{\mathbf{k}>0} v_k e^{-i\mathbf{k}\cdot\left[\mathbf{R}(s)-\mathbf{R}(s')\right]}\right] \times \exp\left[\frac{4}{V}\int_0^{N_1}\mathrm{d}s\int_0^{N_1}\mathrm{d}s' \times \sum_{\mathbf{k}>0} g(k)v_k^2 e^{-i\mathbf{k}\cdot\left[\mathbf{R}(s)-\mathbf{R}(s')\right]}\right] \quad (85)$$

This equation is rewritten as

$$\int \prod_{\mathbf{k}>0}\delta\psi_{\mathbf{k}} e^{-\frac{F_{\mathrm{tot}}}{k_BT}} = \prod_{\mathbf{k}>0}\left(\frac{\pi g(k)}{V}\right) \times \exp\left[-\frac{3}{2\ell^2}\int_0^{N_1}\mathrm{d}s\left(\frac{\partial\mathbf{R}(s)}{\partial s}\right)^2 -\frac{1}{V}\int_0^{N_1}\mathrm{d}s\int_0^{N_1}\mathrm{d}s'\sum_{\mathbf{k}>0} \Delta_k e^{-i\mathbf{k}\cdot\left[\mathbf{R}(s)-\mathbf{R}(s')\right]}\right], \quad (86)$$

where Δ_k is the effective inter-segment interaction given by

$$\Delta_k = v_k - 4g(k)v_k^2. \quad (87)$$

Here, v_k is given by Eq. (26) and $g(k) = V\langle\psi_{\mathbf{k}}\psi_{-\mathbf{k}}\rangle$ is given by Eq. (50).

In the scattering angle limit of $kR_{gi} \gg 1$ (where $i = 1, 2$), relevant to length scales within a polymer chain, and for the high salt limit, $g(k)$ follows from Eq. (74) as

$$g(k) = \frac{12}{\ell^5}\frac{\phi_1\phi_2}{\phi_0}\frac{1}{(k^2+\xi^{-2})}. \quad (88)$$

where (see Eq. (76))

$$\xi^{-2} = \frac{48}{\ell^2}\frac{\phi_1\phi_2}{\phi_0}\frac{w_c}{\kappa^2\ell^3}. \quad (89)$$

Substituting this result in Eq. (87) we obtain

$$\Delta_k = v_k\left[1 - \frac{1}{(1+k^2\xi^2)}\right]. \quad (90)$$

Noting that $v_k = w_c/\kappa^2$ in the present limit, Δ_k follows as

$$\Delta_k = \frac{w_c}{\kappa^2}\left[1 - \frac{1}{(1+k^2\xi^2)}\right]. \quad (91)$$

Upon an inverse Fourier transform, the effective electrostatic interaction between two segments of a labelled chain separated at a distance $\mathbf{r}$, $\Delta(\mathbf{r})$, is given by

$$\Delta(\mathbf{r}) = \frac{w_c}{\kappa^2}\left[\delta(\mathbf{r}) - \frac{1}{4\pi\xi^2}\frac{e^{-r/\xi}}{r}\right]. \quad (92)$$

Thus the inter-segment electrostatic interaction is screened with screening length ξ given by Eq. (89).

7 Size of a labelled chain

Let us identify a single chain of polycations inside a concentrated coacervate. In addition to its conformational entropy due to chain connectivity, any pair of its segments, separated by distance $\mathbf{r}$, interact through the medium with the effective interaction energy $\Delta(\mathbf{r})$ derived above. The probability distribution function for finding its end-to-end distance at $\mathbf{R}$ is given by

$$P(\mathbf{R}) = \int_{\mathbf{0}}^{\mathbf{R}} \mathcal{D}[\mathbf{R}]\exp\left[-\frac{3}{2\ell^2}\int_0^{N_1}\mathrm{d}s\left(\frac{\partial\mathbf{R}(s)}{\partial s}\right)^2 -\frac{1}{2}\int_0^{N_1}\mathrm{d}s\int_0^{N_1}\mathrm{d}s'\Delta[\mathbf{R}(s)-\mathbf{R}(s')]\right] \quad (93)$$

For the specific situation of high enough salt, $\Delta(\mathbf{r})$ is given by Eq. (92).

The mean square end-to-end distance $\langle R^2\rangle$ of the labelled chain can be calculated from $P(\mathbf{R})$ using a variety of calculational procedures such as perturbation theory and variational arguments [2]. The most effective way to calculate $\langle R^2\rangle$ is using a variational procedure, as demonstrated for a single self-avoiding walk chain [2] and polyelectrolyte chains [3]. Instead of reproducing the derivation given in Ref.3 for the generic form of Eqs. (92) and (93), we simply quote the results. From Eqs. (3.49) and (3.50) of Ref. [3], the mean square end-to-end distance of the labelled polycation of N_1 segments is given by

$$\langle R^2\rangle = N_1\ell\ell_1, \quad (94)$$

where the effective chain expansion factor ℓ_1 is given as

$$\ell_1^3\left(\frac{1}{\ell}-\frac{1}{\ell_1}\right)=\frac{12}{\pi\ell^2}\frac{w_c}{\kappa^2}\xi, \tag{95}$$

where ξ is given by Eq. (89). Due to high concentrations ϕ_1 and ϕ_2 of the polycations and polyanions in the coacervate, ξ is small and hence we expect ℓ_1 as only a minor perturbation of the bare segment length ℓ. Therefore, we get from Eq. (95)

$$\left(\frac{1}{\ell}-\frac{1}{\ell_1}\right)=\frac{12}{\pi\ell^5}\frac{w_c}{\kappa^2}\xi, \tag{96}$$

so that

$$\ell_1=\ell\left[1+\frac{12}{\pi\ell^4}\frac{w_c}{\kappa^2}\xi+\cdots\right] \tag{97}$$

Substituting this result in Eq. (94), we get the mean square end-to-end distance of a labelled polycation chain of N_1 segments as

$$\langle R^2\rangle=N_1\ell^2\left[1+\frac{12}{\pi\ell^4}\frac{w_c}{\kappa^2}\xi+\cdots\right] \tag{98}$$

Using Eq. (89) for ξ, we get

$$\langle R^2\rangle=N_1\ell^2\left[1+\left(\frac{12}{\pi}\frac{\alpha^2 z_p^2\ell_B}{\kappa^2\ell^3}\frac{\phi_0}{\phi_1\phi_2}\right)^{1/2}+\cdots\right] \tag{99}$$

Within the framework of the variational procedure used in obtaining the above results for $\langle R^2\rangle$, one of the assumptions is that the chain undergoes uniform swelling. With this assumption, the radius of gyration R_g of the labelled chain is given by the standard result,

$$R_g^2=\frac{\langle R^2\rangle}{6}. \tag{100}$$

Thus, for a labelled polycation chain,

$$\sqrt{\langle R^2\rangle}\sim R_g\sim N_1^{1/2}, \tag{101}$$

so that the size exponent ν is the value of a Gaussian chain,

$$\nu=\frac{1}{2}. \tag{102}$$

The prefactor of the Gaussian chain result, given by the terms inside the square brackets of Eq. (99), increases with a decrease in $\sqrt{c_s}$. In addition, the prefactor is affected by the individual concentrations of polycations and polyanions. These conclusions drawn from Eqs. (98)–(102) are valid for a labelled polyanion as well, by replacing N_1 by N_2.

8 Conclusions

Considering the high polymer concentration regime of coacervates formed by uniformly charged flexible polycations and polyanions in aqueous electrolyte solutions, we present a theory to address correlations of concentration fluctuations, effective electrostatic interaction, structure factor, and radius of gyration of labelled chains. Closed-form formulas are presented for these quantities in terms of the concentration and degree of polymerization of polycations and polyanions, salt concentration, degree of ionization of the polymers, and the Bjerrum length.

Due to the opposite signs of charges on the polycations and polyanions, the net electrostatic energy contribution in the symmetric case of polycation and polyanion concentrations is zero at the mean field level. This implies that the chains are expected to behave like Gaussian chains from the electrostatic point of view. This means that any experimentally observed molecular weight-dependent chain swelling must arise from the short-ranged excluded volume interactions representing the polymer backbone chemistry. However, we show that concentration fluctuations affect the thermodynamics of the system and chain statistics. Even though the size exponent ν is 1/2, as that of a Gaussian chain, the concentration fluctuations lead to chain swelling. The swelling factor is derived to depend on the degree of ionization (α), Bjerrum length (ℓ_B), salt concentration (c_s), and the individual polycation concentration (c_1) and polyanion concentration (c_2), as given in Eq. (99). The swelling factor increases with an increase in $\left(\alpha^2\ell_B/(c_s c_1 c_2)\right)^{1/2}$. Since most of the experiments are performed not at very low salt concentrations, we have provided the above results pertinent to experimentally relevant salt concentrations.

The root cause of the emergence of Gaussian size exponent ($\nu=1/2$) in concentrated coacervates is the screening of electrostatic interaction among all charged segments by the topological correlation of all interpenetrating polyelectrolyte chains. The effective electrostatic interaction energy between two charges in the coacervate is in the same form (Eq. (92)) as for neutral systems and polyelectrolyte solutions [2-8],

$$\Delta(\mathbf{r})\sim\left[\delta(\mathbf{r})-\frac{1}{4\pi\xi^2}\frac{e^{-r/\xi}}{r}\right], \tag{103}$$

where $\mathbf{r}$ is the charge separation distance, and ξ is the electrostatic screening length. Our derivation shows that, in general for coacervates, the screening length depends on the individual concentrations of the polycation and polyanion [Eq. (60)],

$$\frac{\xi}{\ell}\sim\sqrt{\frac{1}{c_1}+\frac{1}{c_2}}. \tag{104}$$

This result is in contrast with that for neutral polymers or polyelectrolytes at high salt condition [2],

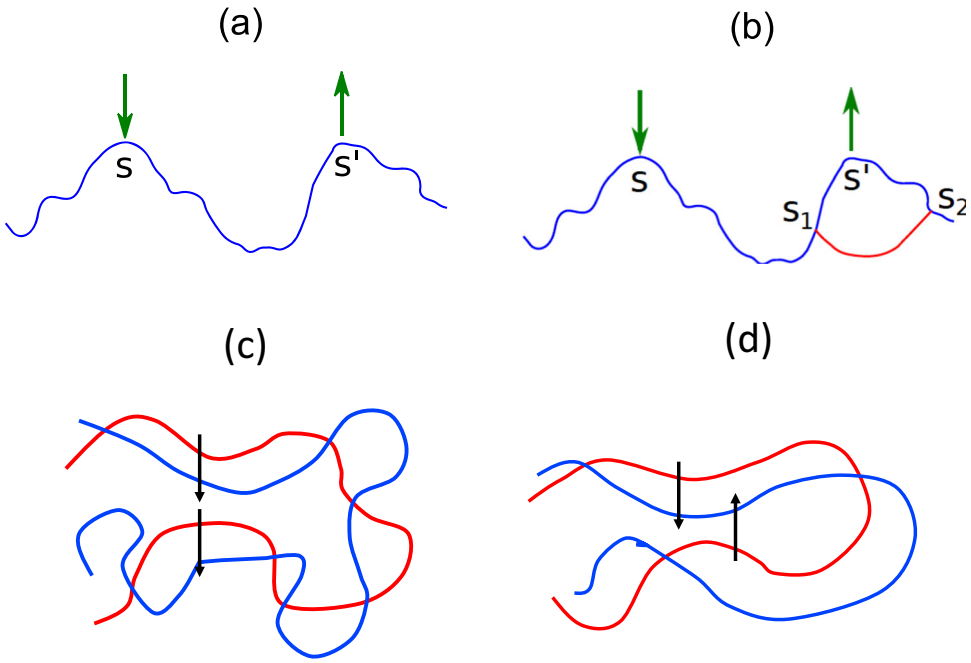

Fig. 4 **a** One-loop polymer diagram used in random phase approximation valid for concentrated coacervates. The monomers s and s' of a polycation or a polyanion chain interact with each other, mediated by the background of all other chains in the system [2]. **b** Higher order correlations are present as vertex diagrams denoting the correlated participation of additional monomers s_1 and s_2 in the interaction between s and s' [2]. **c** Parallel and vertical dipole-dipole interaction of two ion-pairs formed by polycation and polyanion segments. **d** Anti-parallel and horizontal dipole-dipole interaction of two ion-pairs formed by polycation and polyanion segments

$$\frac{\xi}{\ell} \sim \frac{1}{\sqrt{c}}, \tag{105}$$

where c is the polymer concentration.

In terms of connection with scattering experiments, we have identified four regimes: $kR_g \ll 1$, high salt; $kR_g \ll 1$, low salt; $kR_g \gg 1$, high salt; and $kR_g \gg 1$, low salt. In general, for the high salt situation, the scattering intensity follows the Ornstein–Zernike behavior of monotonically decreasing with scattering wave vector. The distinction between the $kR_g \ll 1$ and $kR_g \gg 1$ situations lies only in the temperature-dependent prefactor for the screening length. For low salt conditions, the scattering intensity exhibits a peak at an intermediate scattering wave vector $k^\star$, which depends on the degree of ionization, Bjerrum length, and individual concentrations of polycation and polyanion (Eqs. (69) and (79)),

$$k^\star \ell \sim \left(\frac{\alpha^2 \ell_B}{\ell}\right)^{1/4} \left(\frac{1}{c_1} + \frac{1}{c_2}\right)^{-1/4}, \tag{106}$$

with the prefactor depending on whether the $kR_g \ll 1$ regime or the $kR_g \gg 1$ regime is interrogated in scattering experiments.

The formulas presented in this paper are valid only for concentrated coacervates at higher temperatures where the concentration fluctuations are weak. When the polymer concentration is in the semidilute regime, we have to include additional inter-segment correlations beyond those treated in the random phase approximation (RPA) used in the present derivations. In RPA, only one-loop polymer diagram (Fig. 4a) and its geometric series are accounted for. It is necessary to account for the vertex diagrams such as the one in Fig. 4b to describe the semidilute condition as in the polyelectrolyte solutions [3]. This calculation is relegated to future work.

Furthermore, we expect that ion-pairs formed by two oppositely charged monomers of polycations and polyanions are long-lived at sufficiently lower temperatures. Such ion-pairs can lead to physical associations arising from dipole-dipole interactions as sketched in Fig. 4c, d [70]. These associations result in reduction of conformational entropy of polycations and polyanions and can significantly affect concentration fluctuations and the consequent experimentally measurable quantities. Addressing the interference of physical associations on concentration fluctuations is a difficult task, and is relegated to future.

Acknowledgements Acknowledgement is made to the National Science Foundation (Grant No. DMR 2015935) and AFOSR (Grant No. FA9550-20-1-0142).

Data availability No data associated in this manuscript.

References

1. P.G. de Gennes, P. Pincus, R.M. Velasco, F. Brochard, Remarks on polyelectrolyte conformation. J. Phys. **37**, 1461–1473 (1976)
2. M. Muthukumar, *Physics of Charged Macromolecules: Synthetic and Biological Systems* (Cambridge University Press, Cambridge, 2023)
3. M. Muthukumar, Double screening in polyelectrolyte solutions: limiting laws and crossover formulas. J. Chem. Phys. **105**, 5183–5199 (1996)
4. M. Muthukumar, Electrostatic correlations in polyelectrolyte solutions. Polym. Sci., Ser. A **58**, 852–863 (2016)
5. S.F. Edwards, The theory of polymer solutions at intermediate concentration. Proc. Phys. Soc. **88**, 265–280 (1966)
6. P.G. de Gennes, *Scaling Concepts in Polymer Physics* (Cornell University Press, Ithaca, 1979)
7. M. Doi, S.F. Edwards, *The Theory of Polymer Dynamics* (Clarendon Press, Oxford, 1986)
8. M. Muthukumar, S.F. Edwards, Extrapolation formulas for polymer solution properties. J. Chem. Phys. **76**, 2720–2730 (1982)
9. D.A. McQuarrie, *Statistical Mechanics* (Harper & Row, New York, 1976)
10. S. Förster, M. Schmidt, Polyelectrolytes in solution. Adv. Polym. Sci. **120**(1), 51–133 (1995)
11. M. Muthukumar, A perspective on polyelectrolyte solutions. Macromolecules **50**, 9528–9560 (2017)
12. M. Nierlich, C.E. Williams, F. Boue, J.P. Cotton, M. Daoud, B. Farnoux, G. Jannink, C. Picot, M. Moan, C. Wolff, M. Rinaudo, P.G. de Gennes, Small angle neutron scattering by semi-dilute solutions of polyelectrolyte. J. Phys. **40**, 701–704 (1979)
13. K. Nishida, K. Kaji, T. Kanaya, High concentration crossovers of poly-electrolyte solutions. J. Chem. Phys. **114**, 8671–8677 (2001)
14. Small-angle scattering study, K. Nishida, K. Kaji, T. Kanaya, T. Shibano, T. Added salt effect on the intermolecular correlation in flexible polyelectrolyte solutions. Macromolecules **35**, 4084–4089 (2002)
15. M. Olvera de la Cruz, M.L. Belloni, M. Delsanti, J.P. Dalbiez, O. Spalla, M. Drifford, Precipitation of highly charged polyelectrolyte solutions in the presence of multivalent salts. J. Chem. Phys. **103**, 5781 (1995)
16. I. Sabbagh, M. Delsanti, Solubility of highly charged anionic polyelectrolytes in presence of multivalent cations: specific interaction effect. Eur. Phys. J. E **1**, 75–86 (2000)
17. C.-L. Lee, M. Muthukumar, Phase behavior of polyelectrolyte solutions with salt. J. Chem. Phys. **130**, 018608 (2009)
18. H.G. Bungenberg de Jong, H.R. Kruyt, Coacervation (Partial miscibility in colloid systems, Proc. K. Ned. Akad. Wet., **32**, 849–855 (1929)
19. M. J. Voorn, Complex Coacervation, Rec. trav. chim., 75, Part I (337-330); Part II (405-426); Part III (427–446); Part IV (925–937); Part V (1021-1030) (1956)
20. J.T.G. Overbeek, M.J. Voorn, Phase separation in polyelectrolyte solutions. Theory of complex coacervation. J. Cell. Compar. Physiol. **49**, 7–26 (1957)
21. A. Veis, C. Aranyi, Phase separation in polyelectrolyte systems. I. Complex coacervates of gelatin, J. Phys. Chem., **64**, 1203–1210 (1960)
22. A.S. Michaels, Polyelectrolyte complexes. Ind. Eng. Chem. **57**, 32–40 (1965)
23. E. Tsuchida, Y. Osada, H. Ohno, Formation of interpolymer complexes, J. Macromol. Sci.-Phys. B, **17**, 683–714 (1980)
24. V.A. Kabanov, A.B. Zezin, V.A. Izumrudov, T.K. Bronich, K.N. Bakeev, Cooperative interpolyelectrolyte reactions, Makromol. Chem., Suppl., **13**, 137–155 (1985)
25. B. Philipp, H. Dautzenberg, K.-J. Linow, J. Kötz, W. Dawydoff, Polyelectrolyte complexes-Recent developments and open problems, Prog. Polym. Sci., **14**, 91–172 (1989)
26. J. Kötz, Polyelectrolyte complexes. Polym. Mater. Encycl. **8**, 5762–5770 (1996)
27. V.A. Kabanov, Polyelectrolyte complexes in solution and in bulk. Russ. Chem. Rev. **74**, 3–20 (2005)
28. Z. Ou, M. Muthukumar, Entropy and enthalpy of polyelectrolyte complexation: Langevin dynamics simulations. J. Chem. Phys. **124**, 154902 (2006)
29. X. Wang, Y. Li, Y.-W. Wang, J. Lal, O. Huang, Microstructure of β-lactoglobulin/pectin coacervates studied by small-angle neutron scattering. J. Phys. Chem. B **111**, 515–520 (2007)
30. S. Chodankar, V. Aswal, J. Kohlbrecher, R. Vavrin, A. Wagh, Structural study of coacervation in protein-polyelectrolyte complexes. Phys. Rev. E **78**, 031913 (2008)
31. E. Spruijt, A.H. Westphal, J.W. Borst, M.A. Cohen Stuart, J. van der Gucht, Binodal Compositions of Polyelectrolyte Complexes, Macromolecules, **43**, 6476–6484 (2010)
32. E. Kizilay, A.B. Kayitmazer, P.L. Dubin, Complexation and coacervation of polyelectrolytes with oppositely charged colloids. Adv. Coll. Interface. Sci. **167**, 24–37 (2011)
33. J. van der Gucht, E. Spruijt, M. Lemmers, M.A. Cohen Stuart, Bulk phases and colloidal systems, polyelectrolyte complexes. J. Colloid Interface Sci. **361**, 407–422 (2011)
34. D. Priftis, N. Laugel, M. Tirrell, Thermodynamic characterization of polypeptide complex coacervation. Langmuir **28**, 15947–15957 (2012)
35. Z. Dai, C. Wu, How does DNA complex with polyethylenimine with different chain lengths and topologies in their aqueous solution mixtures? Macromolecules **45**, 4346–4353 (2012)
36. M.Z. Markarian, H.H. Hariri, A. Reisch, V.S. Urban, J.B. Schlenoff, A small- angle neutron scattering study of the equilibrium conformation of polyelectrolytes in stoichiometric saloplastic polyelectrolyte complexes. Macromolecules **45**, 1016–1024 (2012)
37. E. Spruijt, F.A.M. Leermakers, R. Fokkink, R. Schweins, A.A. Van Well, M.A. Cohen Stuart, J. van der Gucht, Structure and dynamics of polyelectrolyte complex coacervates studied by scattering of neutrons, X-rays, and light, Macromolecules, **46**, 4596–4605 (2013)
38. R. Chollakup, J.B. Beck, K. Dirnberger, M. Tirrell, C.D. Eisenbach, Polyelectrolyte molecular weight and salt effects on the phase behavior and coacervation of aqueous solutions of poly(acrylic acid) sodium salt

and poly(allylamine) hydrochloride. Macromolecules **46**, 2376–2390 (2013)
39. J. Qin, D. Priftis, R. Farina, S.L. Perry, L. Leon, J. Whitmer, K. Hoffmann, M. Tirrell, J.J. De Pablo, Interfacial tension of polyelectrolyte complex coacervate phases. ACS Macro Lett. **3**, 565–568 (2014)
40. S.L. Perry, Y. Li, D. Priftis, L. Leon, M. Tirrell, The effect of salt on the complex coacervation of vinyl polyelectrolytes. Polymers **6**, 1756–1772 (2014)
41. Q. Wang, J.B. Schlenoff, The polyelectrolyte complex/coacervate continuum. Macromolecules **47**, 3108–3116 (2014)
42. P.K. Jha, P.S. Desai, J. Li, R.G. Larson, pH and salt effects on the associative phase separation of oppositely charged polyelectrolytes. Polymers **6**, 1414–1436 (2014)
43. D. Priftis, X. Xia, K.O. Margossian, S.L. Perry, L. Leon, J. Qin, J.J. de Pablo, M. Tirrell, Ternary, tunable polyelectrolyte complex fluids driven by complex coacervation. Macromolecules **47**, 3076–3085 (2014)
44. S.L. Perry, L. Leon, K.O. Hoffmann, M.J. Kade, D. Priftis, K.A. Black, D. Wong, R.A. Klein, C.F. Pierce, K.O. Margossian et al., Chirality-selected phase behaviour in ionic polypeptide complexes. Nat. Commun. **6**, 6052 (2015)
45. A. Salehi, P.S. Desai, J. Li, C.A. Steele, R.G. Larson, Relationship between polyelectrolyte bulk complexation and kinetics of their layer-by-layer assembly. Macromolecules **48**, 400–409 (2015)
46. M. Zhao, J. Zhou, C. Su, L. Niu, D. Liang, B. Li, Complexation behavior of oppositely charged polyelectrolytes: effect of charge distribution. J. Chem. Phys. **142**, 204902 (2015)
47. J. Fu, J.B. Schlenoff, Driving forces for oppositely charged polyion association in aqueous solutions: enthalpic, entropic, but not electrostatic. J. Am. Chem. Soc. **138**, 980–990 (2016)
48. M. Radhakrishna, K. Basu, Y. Liu, R. Shamsi, S.L. Perry, C.E. Sing, Molecular connectivity and correlation effects on polymer coacervation. Macromolecules **50**, 3030–3037 (2017)
49. L.-W. Chang, T.K. Lytle, M. Radhakrishna, J.J. Madinya, J. Velez, C.E. Sing, S.L. Perry, Sequence and entropy-based control of complex coacervates. Nat. Commun. **8**, 1–8 (2017)
50. J. Fu, H.M. Fares, J.B. Schlenoff, Ion-pairing strength in polyelectrolyte complexes. Macromolecules **50**, 1066–1074 (2017)
51. H.M. Fares, Y.E. Ghoussoub, J.D. Delgado, J.C. Fu, V.S. Urban, J.B. Schlenoff, Scattering neutrons along the polyelectrolyte complex/coacervate continuum. Macromolecules **51**, 4945–4955 (2018)
52. A.B. Marciel, S. Srivastava, M.V. Tirrell, Structure and rheology of polyelectrolyte complex coacervates. Soft Matter **14**, 2454–2464 (2018)
53. S. Adhikari, M.A. Leaf, M. Muthukumar, Polyelectrolyte complex coacervation by electrostatic dipolar interactions. J. Chem. Phys. **149**, 163308 (2018)
54. S. Adhikari, V.M. Prabhu, M. Muthukumar, Lower critical solution temperature behavior in polyelectrolyte complex coacervates. Macromolecules **52**, 6998–7004 (2019)
55. T.K. Lytle, L.-W. Chang, N. Markiewicz, S.L. Perry, C.E. Sing, Designing electrostatic interactions via polyelectrolyte monomer sequence. ACS Cent. Sci. **5**, 709–718 (2019)
56. J.B. Schlenoff, M. Yang, Z.A. Digby, Q. Wang, Ion content of polyelectrolyte complex coacervates and the Donnan equilibrium. Macromolecules **52**, 9149–9159 (2019)
57. S. Srivastava, M.V. Tirrell, Polyelectrolyte complexation. Adv. Chem. Phys. **161**, 499–543 (2016)
58. C.E. Sing, Development of the modern theory of polymeric complex coacervation. Adv. Coll. Interface. Sci. **239**, 2–16 (2017)
59. C.E. Sing, S.L. Perry, Recent progress in the science of complex coacervation. Soft Matter **16**, 2885–2914 (2020)
60. S.F. Banani, H.O. Lee, A.A. Hyman, M.K. Rosen, Biomolecular condensates: organizers of cellular biochemistry. Nat. Rev. Mol. Cell Biol. **18**, 285–298 (2017)
61. M. Kato, T.W. Han, S. Xie, K. Shi, X. Du, L.C. Wu, H. Mirzaei, E.J. Goldsmith, J. Longgood, J. Pei, N.V. Grishin, D.E. Frantz, J.W. Schneider, S. Chen, L. Li, M.R. Sawaya, D. Eisenberg, R. Tycko, S.L. McKnight, Cell-free formation of RNA granules: low complexity sequence domains form dynamic fibers within hydrogels. Cell **149**, 753–767 (2012)
62. A. Molliex, J. Temirov, J. Lee, M. Coughlin, A.P. Kanagaraj, H.J. Kim, T. Mittag, J.P. Taylor, Phase separation by low complexity domains promotes stress granule assembly and drives pathological fibrillization. Cell **163**, 123–133 (2015)
63. C.W. Pak, M. Kosno, A.S. Holehouse, S.B. Padrick, A. Mittal, R. Ali, A.A. Yunus, D.R. Liu, R.V. Pappu, M.K. Rosen, Sequence determinants of intracellular phase separation by complex coacervation of a disordered protein. Mol. Cell **63**, 72–85 (2016)
64. A. Borgia, M.B. Borgia, K. Bugge, V.M. Kissling, P.O. Heidarsson, C.B. Fernandes, A. Sottini, A. Soranno, K.J. Buholzer, D. Nettels, B.B. Kragelund, R.B. Best, B. Schuler, Extreme disorder in an ultrahigh-affinity protein. Nature **555**, 61–66 (2018)
65. K.M. Ruff, R.V. Pappu, A.S. Holehouse, Conformational preferences and phase behavior of intrinsically disordered low complexity sequences: insights from multiscale simulations. Curr. Opin. Struct. Biol. **56**, 1–10 (2019)
66. J.-M. Choi, A.S. Holehouse, R.V. Pappu, Physical principles underlying the complex biology of intracellular phase transitions. Annu. Rev. Biophys. **49**, 107–133 (2020)
67. S. Das, M. Muthukumar, Microstructural organization in α-synuclein solutions. Macromolecules **55**, 4228–4236 (2022)
68. S. Mukherjee, A. Sakunthala, L. Gadhe, M. Poudyal, A.S. Sawner, P. Kadu, S.K. Maji, J. Mol. Biol. **435**, 167713 (2023)
69. C. Duan, R. Wang, Phys. Rev. Lett. **130**, 158401 (2023)
70. M. Muthukumar, Localized structures of polymers with long-range interactions. J. Chem. Phys. **104**, 691–700 (1996)